Journal of Orthopaedic Research

Journal of Orthopaedic Research®

RESEARCH ARTICLE

Electrophoretic Deposition of Gentamicin Into Titania Nanotubes Prevents Evidence of Infection in a Mouse Model of Periprosthetic Joint Infection

John L. Hamilton[1] | Sofia Gianotti[1] | Julia Fischer[1] | Greta Della Fara[1] | Amandine Impergre[1] | Francesca De Vecchi[1] | Mohammed AbuAlia[1] | Alfons Fischer[1,2] | Adrienn Markovics[1] | Markus A. Wimmer[1]

[1]Department of Orthopedic Surgery, Rush University Medical Center, Chicago, Illinois, USA | [2]Department of Microstructure Physics and Alloy Design, Max-Planck-Institute for Sustainable Materials, Duesseldorf, Germany

Correspondence: John L. Hamilton (John_L_Hamilton@rush.edu)

Received: 5 September 2024 | **Revised:** 15 November 2024 | **Accepted:** 4 December 2024

Funding: This study was funded by the Grainger Directorship of the Rush Arthritis and Orthopedics Institute, NIH NIAMS R21 grant (R21AR084167), and NIH NIAMS T32 grant (T32AR073157).

Keywords: electrophoretic deposition | implant-associated infection | periprosthetic joint infection | *Staphylococcus aureus* | titania nanotubes

ABSTRACT

Periprosthetic joint infection (PJI) is a leading cause and major complication of joint replacement failure. As opposed to standard-of-care systemic antibiotic prophylaxis for PJI, we developed and tested titanium femoral intramedullary implants with titania nanotubes (TNTs) coated with the antibiotic gentamicin and slow-release agent chitosan through electrophoretic deposition (EPD) in a mouse model of PJI. We hypothesized that these implants would enable local gentamicin delivery to the implant surface and surgical site, effectively preventing bacterial colonization. In the mouse PJI model, C57BL/6 mice received implants with TNTs coated with chitosan (chitosan group; control group) or with TNTs coated with chitosan and gentamicin (chitosan + gentamicin group; experimental group). Following implant placement, the surgical site was inoculated with 1×10^3 CFUs of Xen36 bioluminescent *Staphylococcus aureus*. All the mice in the chitosan group and none in the chitosan + gentamicin group had evidence of infection based on CFU analysis and bioluminescence imaging through the 14-day assessment postsurgery. Correspondingly, scanning electron microscopy analysis at the implant surface demonstrated bacterial biofilm only in the chitosan group. Furthermore, periosteal reaction and peri-implant bone loss at the femur were significantly reduced in the chitosan + gentamicin group. The chitosan + gentamicin group had reduced pain behavior, improved weight-bearing, and increased weight compared to the chitosan-control group. This study provides preclinical evidence supporting the efficacy of implants with TNTs coated with chitosan and gentamicin through EPD for preventing bacterial colonization and biofilm formation in a mouse model of PJI.

1 | Introduction

Periprosthetic joint infection (PJI) refers to infection occurring on and around a joint replacement implant; bacterial infections comprise the vast majority of cases, of which *Staphylococcus aureus* is one of the most common causative organisms identified [1–6]. PJI is the leading cause of modern joint replacement failure [7] and occurs in approximately 1%–2% of primary total joint arthroplasties [6, 8, 9], and reported rates can eclipse 9% in revision total joint arthroplasties [10–12]. Furthermore, PJI is a devastating complication that is difficult to treat and is associated with significant morbidity and mortality [13–15]. The 5-year mortality of patients with PJI is approximately 20%, similar to many common cancers [14, 15]. By 2030, in the United States alone, the total number of annual

cases of PJI with total hip and knee arthroplasty is projected to be over 65,000, with an estimated annual hospital cost of $1.85 billion [16].

There is a crucial need for improved strategies to prevent PJI. Clinically used peri-operative systemic antibiotics are limited by low local bioavailability at the implant and surgical site—this limitation could be overcome by utilizing an implant antimicrobial coating. To date, different clinically used orthopedic implant coatings have included gentamicin poly (D, L-lactide), silver, and povidone-iodine coatings [17]. However, among these technologies, there is limited clinical development for an implant antimicrobial coating for PJI prevention. We developed and tested a modified implant with an antimicrobial coating for PJI prevention. Specifically, we created titanium (Ti) implants featuring a titania nanotube (TNT) surface that was coated with the antibiotic gentamicin and the slow-release agent chitosan through electrophoretic deposition (EPD) [18].

Ti and its alloys are recognized as implant materials due to their superb biocompatibility, suitable elasticity, and high corrosion resistance [19]. Ti can spontaneously form a stable and inert layer of titanium oxide [20]. When the oxide layer is manipulated at the nanoscale, nanotubes can be created [21]. TNTs can increase the surface area and create pockets for drug loading and delivery [18, 22]. Additionally, the enhanced surface area and nanotubular architecture generated by TNTs can lead to increased titanium-bone contact across a larger area, promoting enhanced osseointegration [23–26].

We previously demonstrated that applying a cathodic potential to Ti implants with TNTs can effectively create a coating of the antibiotic gentamicin and the slow-release agent chitosan on the implant surface [18]. EPD enables the deposition of a therapeutic agent onto the implant surface within a few minutes [18]. Coating the implant with an antibiotic serves two primary functions: (i) preventing colonization and bacterial biofilm formation on the implant surface and (ii) allowing the implant to act as an antimicrobial drug delivery device to the surrounding tissue.

In this investigation, we assessed Ti implants with TNTs coated with gentamicin and chitosan in a well-established mouse model of PJI [27–34] using inoculation with *S. aureus* at the time of implant surgery. We monitored for bacterial presence and secondary markers associated with infection over 14 days post-surgery. We hypothesized that Ti implants with TNTs coated with gentamicin and chitosan would prevent bacterial colonization at the implant and surgical site over 14 days.

2 | Methods

2.1 | Creation of TNTs on the Implant Surface

Medical grade titanium (Ti-6Al-4V) wires (0.6 mm diameter and 30 mm length) were obtained from Custom Wire Technologies. The creation of TNTs on the Ti wire surface was performed using an anodization process in the presence of ammonium-fluoride, as previously described [18]. In brief, a two-step anodization procedure—1 h at 70 volts (V), followed by 15 min sonication in methanol, and an additional 30 min at 70 V—was used to create TNTs; this process creates TNTs of approximately 100 nm diameter and 7 μm length [18]. The morphology of the nanotubes was imaged using a JEOL JSM-IT500HR Scanning Electron Microscope (SEM).

2.2 | EPD of Gentamicin and Chitosan Onto the Implant TNT Surface

Ti wires with TNTs were coated with either chitosan alone or a combination of chitosan and gentamicin using EPD, as previously described [18]. Briefly, an Interface 1010E potentiostat (Gamry Instruments) in a two-electrode setup was employed, with the Ti wire serving as the cathode and a spiral-shaped platinum wire as the anode. For the EPD of chitosan onto the Ti wire surface, a one-step process was conducted by applying a potential difference of −5 V for 5 min in a solution of 2 mg/mL chitosan (Sigma-Aldrich; 448869) [18]. Before EPD, the chitosan was crosslinked with sodium tripolyphosphate [18].

For the EPD of chitosan and gentamicin onto the Ti wire surface, a two-step process was utilized. In the first step, a solution containing both 100 mg/mL of gentamicin sulfate (Sigma-Aldrich; G1914) and crosslinked chitosan (2 mg/mL) was used with a potential difference of −5 V for 5 min. In the second step, 2 mg/mL of crosslinked chitosan was applied with a potential difference of −5 V for 5 min. This two-step EPD process yields a mean of 501.5 μg of gentamicin coating on the implant surface [18]. In prior in vitro studies, EPD of chitosan and gentamicin produced a cumulative gentamicin release of 400–550 μg from the implant, as determined through fractional volume sampling over 3 days. Drug release was primarily diffusion-driven, exhibiting an initial burst phase followed by a sustained, slower release of gentamicin over a 3-day assessment period [18].

2.3 | Mouse Model of PJI

This research received approval from the Rush University Medical Center Institutional Animal Care and Use Committee (IACUC No: 23-012). All procedures adhered to the standards outlined in the Guide for the Care and Use of Laboratory Animals (Institute of Laboratory Animal Resources, National Academy of Sciences, Bethesda, MD, USA). A well-established mouse PJI model was used, as previously detailed [27–34]. Before surgery, the right hindlimb of 12-week-old C57BL/6J male mice (Jackson Laboratories) underwent hair removal with the aid of an electric hair clipper and Nair hair removal cream. Baseline measurements were taken for bioluminescence imaging (BLI), pain behavior, and weight-bearing.

On the day of surgery, mice were provided subcutaneous (SC) buprenorphine (0.1 mg/kg) analgesic, anesthetized using 2% isoflurane, and weighed. Surgery was performed using aseptic methods with the aid of a stereomicroscope (Zeiss, Stemi 508), as previously described [27]. An incision was made on the skin above the right knee. A medial parapatellar arthrotomy was performed. The quadriceps-patellar complex was laterally displaced to expose the femoral condyles and intercondylar notch. A 25-gauge syringe needle was utilized to create a hole in the trochlear groove and ream the distal intramedullary canal of the femur. Prepared Ti implants with TNTs coated with chitosan or chitosan + gentamicin that were cut to a length of 7 mm were inserted retrogradely into

the intramedullary canal of the femur using a pin holder (Fine Science Tools, 26018-17), leaving 1 mm exposed outside of the bone.

Following implant placement and with the knee joint surgical site exposed, 1×10^3 CFUs of Xen36 *S. aureus* in a 2 μL solution was administered dropwise, using a 5 μL Hamilton microliter syringe, directly on top of the exposed distal implant [27]. Inoculation with 1×10^3 CFUs of Xen36 *S. aureus* has consistently provided chronic infection in this mouse PJI model [27, 30, 34, 35], for as long as a 42-day assessment [34]. The quadriceps-patellar complex was repositioned to the midline. The knee joint capsule was closed with 6-0 VICRYL sutures (Ethicon), and 6-0 PROLENE sutures (Ethicon) were used for skin closure. An X-ray was performed for each mouse to confirm femoral implant placement.

Post-surgery, specific outcome assessments included BLI on Days 1, 3, 5, 7, 10, and 14, X-ray (Day 14), pain behavior (Days 3 and 14), weight-bearing (Days 3 and 14), and weight change between Day 0 and Day 14. Mice were killed on Day 3 for colony-forming unit (CFU) analysis at the implant and tissue, as well as on Day 14 for CFU analysis at the implant and tissue, SEM at the implant, and histological analysis at the tissue. Additionally, mice were monitored daily for signs of general pain and distress, as outlined in Supplementary Methods S1. Per our IACUC protocol, euthanasia was planned at any time point for any mouse exhibiting severe pain or distress.

All mice received inoculation at the open surgical site with Xen36 *S. aureus*. The control implant group had implants with TNTs coated with chitosan through EPD, which were labeled as the chitosan group. The experimental implant group received implants with TNTs coated with gentamicin and chitosan through EPD, which were termed the chitosan + gentamicin group. A total of 30 mice underwent implant placement: $n = 15$ chitosan group, $n = 15$ chitosan + gentamicin group. On Day 3, $n = 6$ mice from each of the two groups were harvested for CFU analysis, having received BLI up to Day 3. The remaining mice ($n = 9$ chitosan group and $n = 9$ chitosan + gentamicin group) were assessed with BLI up to Day 14, as well as pain behavior and weight-bearing (Days 3 and 14), X-ray (Day 14), and weight change (Day 14). These mice were then harvested on Day 14 for CFU analysis ($n = 6$ per group), as well as SEM analysis at the implant and histologic analysis at the tissue ($n = 3$) per group.

For all studies, the primary outcome was the evaluation of bacteria at the tissue and implant by CFU analysis on Day 3 and Day 14. The remaining assessments were secondary experimental outcomes. Studies were reported in adherence to the ARRIVE guidelines (Animal Research: Reporting of In Vivo Experiments) [36].

2.4 | Preparation of Bacteria

This study utilized bioluminescent Xen36 *S. aureus* (Perkin Elmer), as previously utilized in the mouse model of PJI [27, 29–31, 33, 34]. Bacterial cultures of Xen36 *S. aureus* were grown overnight in tryptic soy broth (TSB) the day before surgery. Directly before surgery, *S. aureus* was diluted in TSB to achieve an optical density of 0.5 at 600 nm, as measured with a spectrophotometer against a TSB blank; this corresponds to approximately 1.0×10^8 CFU/mL. This bacterial suspension was then further diluted to 5×10^5 CFU/mL in PBS. During the surgical procedure, following implant placement, 2 μL of the 5×10^5 CFU/mL of bacterial solution was inoculated at the surgical site with a 5 μL Hamilton syringe, delivering a total of 1×10^3 CFUs to the knee joint surgical site.

2.5 | BLI

BLI was conducted using the IVIS Lumina II In Vivo Imaging System (Perkin Elmer), as previously described [27]. The intensity of the *S. aureus* bioluminescent signal directly correlates with the bacterial burden quantified by CFU count in the mouse PJI model [28]. For BLI, a 5-min exposure time was utilized. For quantitative assessment of the bioluminescent signal, a standard circular region of interest (ROI) was used, covering the distal 1/4th of the femur and the proximal 1/4th of the tibia/fibula, and quantification was performed by assessing average radiance (photons/s/cm^2/sr) at the ROI [27]. Imaging was performed under 2% isoflurane anesthesia.

2.6 | CFU Assay

The distal 1/4th of the femur and the proximal 1/4th of the tibia/fibula were cut from the right hindlimb to harvest the knee joint [27]. The bone and soft tissue of the knee joint, excluding the skin, were utilized for CFU analysis. The implant was carefully removed from the femur. The knee joint bone and soft tissue and implant were placed in separate Eppendorf tubes in 6 mg/mL collagenase D solution. Using sterile, straight, fine-tipped scissors, the tissue was dissected into pieces of approximately 1 mm directly within the tubes. The tissue and implants underwent a 30-second cycle of high-speed vortexing, followed by a 15-min incubation at 37°C. This process was repeated with an additional 30-s vortex cycle and a 15-min incubation at 37°C. CFU counts from processed tissues and implants were measured using serial dilution and plating techniques, as detailed previously [27, 37–41]. Serial dilutions in PBS that ranged from 10^{-1} to 10^{-5} in 96-well microplates were performed. Aliquots (10 μL) were spot-plated on tryptic soy agar plates and incubated at 37°C overnight. The following day, CFU counts were quantified. Bacterial burden was expressed as CFU per gram (g) of tissue and CFU per implant [27].

2.7 | Histology

Preparation of femur tissue for histologic analysis was performed as previously described [27].

The tissue was harvested and fixed in 4% formaldehyde for 3 days at 4°C, followed by storage in 70% ethanol at 4°C. The tissue underwent decalcification in 0.5 M EDTA (pH 8.0) at 4°C for 14–21 days, followed by embedding in paraffin. Serial 5 μm sagittal sections were prepared and stained with hematoxylin and eosin (H&E). These sections were imaged using an Olympus BX43 light microscope.

2.8 | Weight-Bearing

Mice were recorded for weight-bearing at the implant leg using slow-motion video software on an iPhone 14 [27, 42]. The

grading system for the right hindlimb is the following: full weight-bearing (three points), partial weight-bearing (two points), toe-touch (one point), and nonweight-bearing (0 points). Scoring was conducted by two blinded observers, yielding a high intraclass correlation coefficient (ICC) of 0.98 with a 95% confidence interval (CI) of 0.96–0.99. The mean score between two blinded observers was used for each mouse.

2.9 | Pain Behavior

To evaluate pain behavior at the implant leg, mechanical allodynia was evaluated using von Frey filament testing [27, 43, 44]. Mice were positioned on an IITC mesh stand (part# 408) inside a small plastic enclosure. Calibrated von Frey monofilaments (Stoelting Touch Test Sensory Evaluator Kit), ranging from filament forces of 2.44–4.74 grams-force, were used to assess the response. The monofilaments were gently pressed against the plantar surface of the right hind paw with sufficient force to bend the monofilament for 3 s or until a pain response was observed. A modified up-down method was utilized to quantify the paw withdrawal threshold force in g [27, 43, 44].

2.10 | Weight

Mice were weighed directly before surgery and again on Day 14 postsurgery. Weight was measured in g using an electronic balance (Ohaus, Scout SPX). Change in weight from baseline to Day 14 was assessed between groups.

2.11 | Radiography

Mice underwent X-ray imaging under 2% isoflurane anesthesia using a KUBTEC PARAMETER X-ray Cabinet directly after implant placement and on Day 14. Radiographic scoring criteria were modified based on what we have previously described [27] and discussed by others [42, 45]. Scores for periosteal reaction and peri-implant bone loss were determined on a scale of 0–2. A score of 2 represented the worst or most severe score, and 0 represented no or minimal pathology. Further details on scoring criteria for a score of 0–2 are provided in Supporting Information S2: Tables S1 and S2. Scoring was performed by two blinded observers. There was a high ICC between the two blinded observers for periosteal reaction (ICC = 0.98; 95% CI of 0.95–0.99) and peri-implant bone loss (ICC = 0.94; 95% CI 0.84–0.98). The mean score between the two blinded observers was used for each radiographic assessment. The mean score for periosteal reaction and peri-implant bone loss was added together to calculate a total radiographic PJI score.

2.12 | SEM

The preparation of implants for SEM was adapted from previous investigations [46–48]. Implants were harvested and rinsed in phosphate-buffered saline (PBS) and underwent fixation with 2% glutaraldehyde/PBS at 4°C for 2 h, rinsed in PBS, and then treated with 1% osmium tetroxide/PBS for 1 h. Implants were then rinsed in PBS, followed by dehydration in an ethanol series, and were then placed in hexamethyldisilazane for 10 min. Implants were stored in a desiccator overnight, prepared with gold sputtering, and imaged using a JEOL JSM-IT500HR SEM.

2.13 | Statistical Analysis

For longitudinal BLI data that combined data from mice harvested from both Day 3 and Day 14, a mixed effects analysis with Bonferroni's correction for multiple comparisons was performed. For longitudinal pain-behavior and weight-bearing data that evaluated only the mice harvested at Day 14, repeated measures two-way analysis of variance (ANOVA) with Bonferroni's correction for multiple comparisons was performed. To assess the presence or absence of bacteria, a chi-square test was planned unless an expected cell count was less than 5, in which a Fisher's exact test was performed. For the remaining assessments, tests for normality were performed with a Shapiro–Wilk test. Normally distributed data was evaluated using an unpaired *t*-test. Non-normally distributed data was analyzed using a Mann–Whitney *U* test. For pain behavior, weight-bearing, and x-ray scoring using two blinded observers, statistical analysis for the ICC was conducted using SPSS Statistics software version 29. Prism software version 10 was used to perform the remaining analyses. Data are presented as mean ± SD. A $p \leq 0.05$ was set as the threshold for statistical significance.

3 | Results

The presence of TNTs, as well as the successful deposition of chitosan or chitosan + gentamicin on the implants following the EPD coating procedure, was confirmed with SEM (Figure 1A–C). The placement of the femoral intramedullary implant is illustrated in Figure 1D. An overview of the evaluation of bacterial presence and secondary infection markers in the mouse PJI model is provided in Figure 1E–L. No deaths or indications of severe pain or distress necessitating euthanasia, as outlined in Supplementary Methods S1, were observed in either group. Correspondingly, no animals were excluded from the study, and the assessments were conducted as outlined.

3.1 | Implants With TNTs Coated With Chitosan and Gentamicin Prevent Evidence of Infection on BLI and CFU Analysis

In the chitosan group, an increase in bioluminescent signal from Xen36 *S. aureus* was observed at the surgical implant and inoculation site from Days 1 to 14, peaking on Day 3 (Figure 2A,B). Conversely, the chitosan + gentamicin group exhibited no increase in bioluminescence signal above baseline throughout the 14-day period (Figure 2A,B). Quantitative analysis of bioluminescence signal intensity revealed significant differences between the chitosan and the chitosan + gentamicin groups on Days 1, 3, and 5 (Figure 2B).

At Day 3, the chitosan + gentamicin group, as compared to the chitosan group, exhibited lower CFU counts in both the tissue

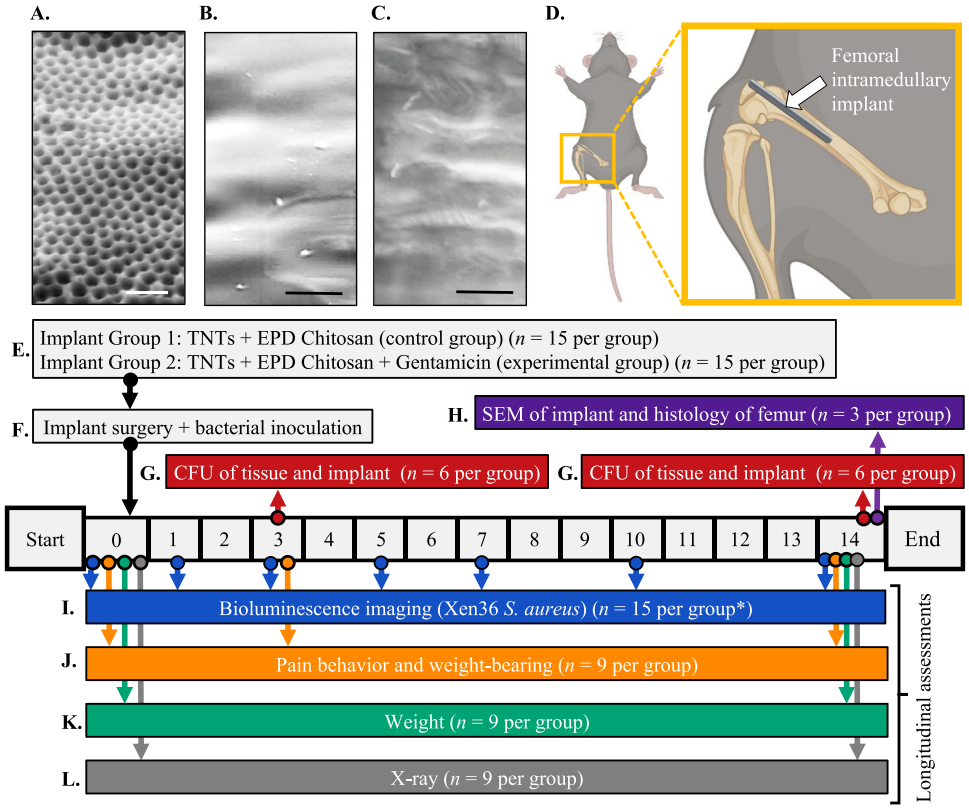

FIGURE 1 | Study overview: (A) Implant with TNTs without coating; (B) Implant with TNTs and electrophoretic deposition (EPD) of chitosan; (C) Implant with TNTs and EPD of chitosan + gentamicin; (D) Illustration of mouse with surgically placed femoral intramedullary implant; (E) Control group received implants with TNTs and EPD of chitosan, while the experimental group received implants with TNTs and EPD of chitosan + gentamicin; (F) Implants were surgically placed in the femoral intramedullary canal, and the surgical site was inoculated with 1×10^3 CFU of Xen36 *S. aureus*; (G) CFU analysis of the tissue and implant was performed at Days 3 and 14; (H) SEM analysis for implant biofilm was conducted at Day 14; (I) Bioluminescence imaging for bioluminescent Xen36 *S. aureus* was performed at baseline and on Days 1, 3, 5, 7, 10, and 14. *There were $n = 15$ mice available per group for bioluminescence imaging until Day 3 harvest for CFU analysis, which was reduced to $n = 9$ available mice per group thereafter; (J) Pain behavior and weight-bearing tests were conducted at baseline, Day 3, and Day 14; (K) Weight was measured at baseline and Day 14; (L) X-ray imaging of the femoral implant and surrounding tissue was performed following implant placement at baseline and at Day 14. White scale bar = 0.5 μm; black scale bars = 2 μm.

(0.00 ± 0.00 CFUs vs. $2.93 \times 10^5 \pm 1.72 \times 10^5$ CFUs; $p < 0.01$) (Figure 2C) and on the implant (0.00 ± 0.00 CFUs vs. $1.12 \times 10^3 \pm 1.08 \times 10^3$ CFUs; $p < 0.01$) (Figure 2D). At Day 3, the presence of any bacteria was lower in the chitosan + gentamicin group as compared to the chitosan group, both in tissue (0/6 vs. 6/6; $p < 0.01$) and on the implant (0/6 vs. 6/6; $p < 0.01$) (Figure 2E). At Day 14, these findings continued with the chitosan + gentamicin group showing lower CFU counts compared to the chitosan group, both in tissue (0.00 ± 0.00 CFUs vs. $8.43 \times 10^4 \pm 1.96 \times 10^5$ CFUs; $p < 0.01$) (Figure 2F) and on the implant (0.00 ± 0.00 CFUs vs. $3.48 \times 10^2 \pm 3.25 \times 10^2$ CFUs; $p = 0.016$) (Figure 2G). Furthermore, the presence of any bacteria remained markedly lower in the chitosan + gentamicin group compared to the chitosan group, both in tissue (0/6 vs. 6/6; $p < 0.01$) and on the implant (0/6 vs. 6/6; $p < 0.01$) (Figure 2H).

3.2 | Implants With TNTs Coated With Chitosan and Gentamicin Prevent Bone Pathology on Radiography and Histology

The chitosan-control group exhibited an increased presence and severity of periosteal reaction and peri-implant bone loss at the distal femur implant site on X-ray imaging on Day 14 (Figure 3A). Radiographic scoring, with scores ranging up to two for the most severe cases, indicated that the severity of periosteal reaction was significantly higher in the chitosan-control group as compared to the chitosan + gentamicin group (1.39 ± 0.86 vs. 0.22 ± 0.44; $p < 0.01$). Additionally, radiographic scoring for peri-implant bone loss was higher in the chitosan group (0.83 ± 0.79 vs. 0.06 ± 0.17; $p = 0.016$) (Figure 3B). The combined PJI score was also higher in the chitosan-control group than in the chitosan + gentamicin group (2.22 ± 1.56 vs. 0.28 ± 0.44; $p = 0.012$) (Figure 3B). On histologic analysis, at Day 14, severe bone loss and corresponding severe inflammatory infiltrate at the distal femur were evident in the chitosan group (Figure 4A left, marked by *), which was not present in the chitosan + gentamicin group (Figure 4A right).

3.3 | Implants With TNTs Coated With Chitosan and Gentamicin Prevent Evidence of Biofilm on the Implant Surface

In the chitosan group, SEM imaging of the distal implant revealed distinct areas of ~0.5–1.5 μm spheres covered and

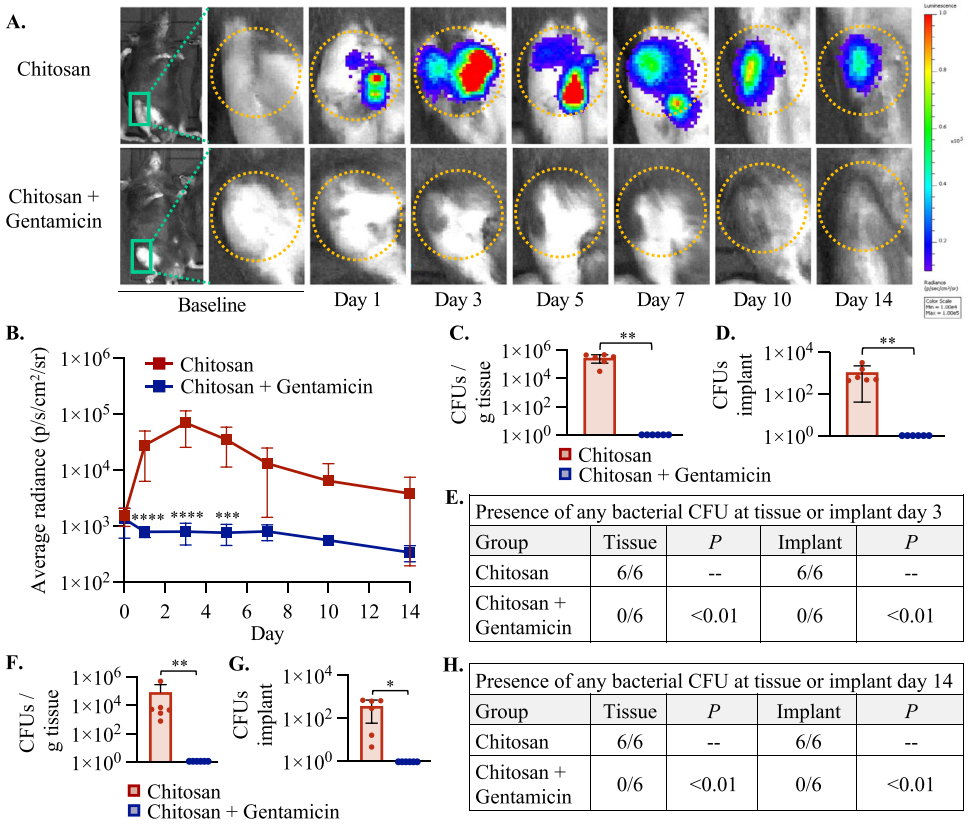

E.

Presence of any bacterial CFU at tissue or implant day 3				
Group	Tissue	*P*	Implant	*P*
Chitosan	6/6	--	6/6	--
Chitosan + Gentamicin	0/6	<0.01	0/6	<0.01

H.

Presence of any bacterial CFU at tissue or implant day 14				
Group	Tissue	*P*	Implant	*P*
Chitosan	6/6	--	6/6	--
Chitosan + Gentamicin	0/6	<0.01	0/6	<0.01

FIGURE 2 | Implants with TNTs Coated with Chitosan and Gentamicin Prevent Evidence of Infection on BLI and CFU Analysis. (A) BLI for bioluminescent Xen36 *Staphylococcus aureus*. Orange dashed circles represent the region of interest at the knee joint used for quantification of the bioluminescent signal. (B) Quantification of bioluminescent signal at the region of interest at the knee joint. (C, D) CFU quantification at the tissue and implant at Day 3. Values of 0 were represented as 1×10^0 to conform to the log scale axis. (E) Presence or absence of bacterial CFUs at the tissue or implant at Day 3. (F, G) CFU quantification at the tissue and implant at Day 14. Values of 0 were represented as 1×10^0 to conform to the log scale axis. (H) Presence or absence of bacterial CFUs at the tissue or implant at Day 14. Data are represented as mean ± SD; $*p < 0.05$, $**p < 0.01$, $***p < 0.001$, $****p < 0.0001$.

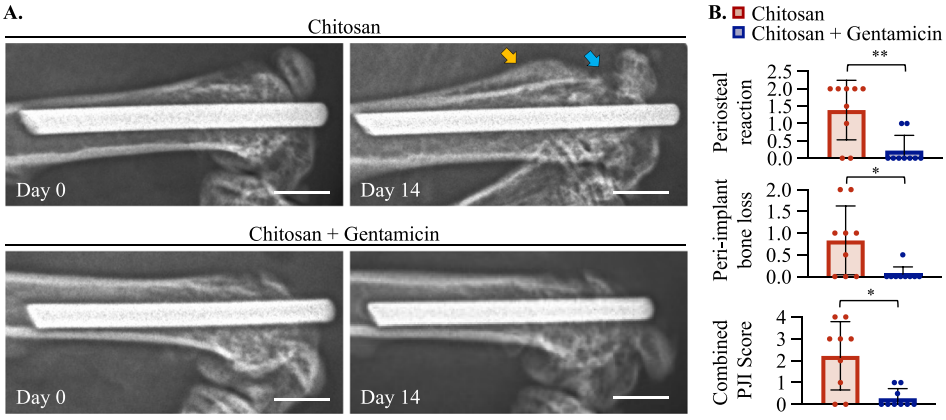

FIGURE 3 | Implants with TNTs coated with chitosan and gentamicin prevent bone-infection associated pathology on radiography: (A) X-ray of the femur and femoral implant at Day 0 and Day 14. The orange arrow highlights the periosteal reaction, and the blue arrow highlights peri-implant bone loss; (B) Radiographic scoring at Day 14 for periosteal reaction, peri-implant bone loss, and combined PJI score (combined periosteal reaction and peri-implant bone loss score). White scale bar = 1.5 mm. Data are represented as mean ± SD; $*p < 0.05$, $**p < 0.01$.

connected by an extracellular matrix characteristic of *S. aureus* biofilm at Day 14. The highest amount of biofilm was identified covering the exposed TNT surface (Figure 4B). Regions of residual chitosan coating were also observed on the distal implant surface (Figure 4B). In contrast, in the chitosan + gentamicin group, characteristic bacterial biofilm was not identified on the distal implant surface, neither on the TNT surface nor on the residual chitosan layer (Figure 4B).

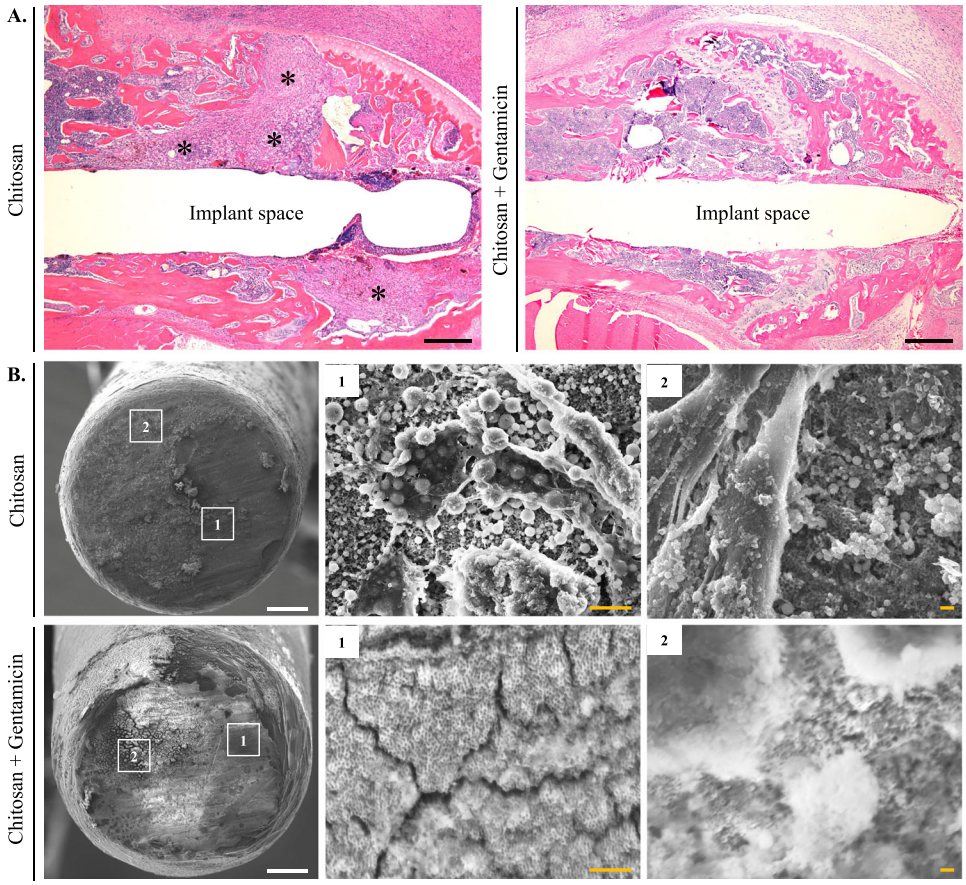

FIGURE 4 | Implants with TNTs coated with chitosan and gentamicin prevent bone-infection associated pathology on histology and prevent evidence of biofilm on the implant surface on SEM: (A) Representative images of paraffin-embedded distal femurs with implants removed and H&E staining. *Regions of substantial inflammatory infiltrate into the bone surrounding the implant, which were present in the chitosan group but not seen in the chitosan + gentamicin group. (B) Representative SEM images of the distal implants with magnified views of a region with bare titanium nanotubes (1) and residual chitosan coating (2). Bacterial biofilms were identified in the chitosan group implants as ~0.5–1.5 μm spheres representing *Staphylococcus aureus* and extracellular matrix connecting and covering the bacteria, which was not identified in the chitosan + gentamicin group implants. Black scale bars = 500 μm; white scale bars = 100 μm; orange scale bars = 2 μm.

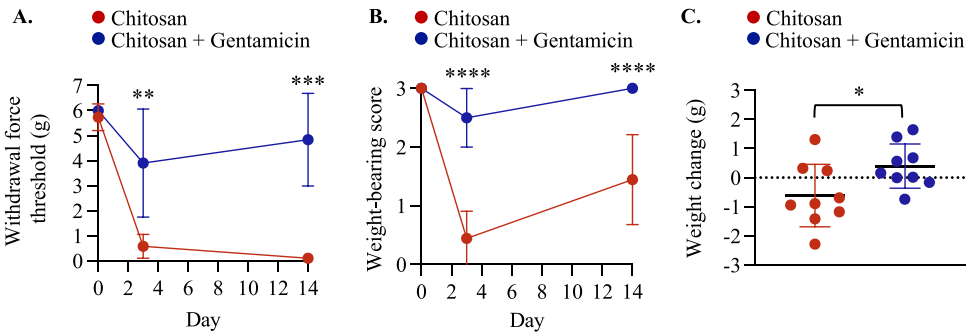

FIGURE 5 | Implants with TNTs coated with chitosan and gentamicin reduced pain behavior, increased weight-bearing, and reduced weight loss: (A) Pain behavior (mechanical allodynia) assessed with von Frey filament testing; (B) Weight-bearing score at the implant leg; (C) Change in weight between Day 0 (baseline) and Day 14; Data represented by mean ± SD; *$p < 0.05$, **$p < 0.01$, ***$p < 0.001$, ****$p < 0.0001$.

3.4 | Implants With TNTs Coated With Chitosan and Gentamicin Reduced Pain Behavior and Increased Weight-Bearing

The chitosan group exhibited greater pain behavior (mechanical allodynia) compared to the chitosan + gentamicin group, as evidenced by lower withdrawal force thresholds on von Frey filament testing at both Day 3 (0.58 ± 0.48 g vs. 3.91 ± 2.16 g; $p < 0.01$) and Day 14 (0.11 ± 0.09 g vs. 4.84 ± 1.85 g; $p < 0.001$) (Figure 5A). The chitosan group exhibited significantly worse (lower) weight-bearing scores compared to the chitosan + gentamicin group at both Day 3 (0.44 ± 0.46 vs. 2.50 ± 0.50; $p < 0.0001$) and Day 14 (1.44 ± 0.77 vs. 3.00 ± 0.00; $p < 0.0001$). At Day 14, all mice in the

chitosan + gentamicin group had a score of 3, representing full weight-bearing (Figure 5B).

3.5 | Implants With TNTs Coated With Chitosan and Gentamicin Reduced Weight Loss

At baseline, directly before surgery, the chitosan group weighed similarly to the chitosan + gentamicin group (27.54 ± 1.31 g vs. 28.10 ± 1.55 g; $p = 0.42$). By Day 14 postsurgery, the chitosan group lost 0.61 ± 1.07 g, and the chitosan + gentamicin group gained 0.40 ± 0.77 g. The difference in weight change between the groups was statistically significant ($p = 0.035$) (Figure 5C).

4 | Discussion

About half of hospital-acquired infections in the United States are associated with indwelling devices, with surgical implant infections, such as joint prostheses, being particularly challenging to manage [49]. PJI is now the leading cause of joint replacement failure [7]. Biofilm formation, which protects bacteria from antimicrobial agents and the immune response, contributes to persistent infections around surgical implants [49, 50]. In this study, implants with TNTs coated with chitosan and gentamicin via EPD prevented bacterial colonization and biofilm formation at the implant and surgical site in a mouse PJI model with *S. aureus* inoculation at the surgical site. Our findings demonstrate an implant and coating technology in an animal model that may effectively prevent peri-operative infection. This approach has the potential to reduce hospital-acquired infections associated with surgical implants, such as joint prostheses.

Based on the CFU assays on Days 3 and 14, mice receiving implants with TNTs coated with chitosan and gentamicin showed no CFUs cultured from the implant or surrounding tissue. Yang et al. demonstrated, using a rat femoral implant-associated infection model with *S. aureus*, that implants with TNTs coated with gentamicin via a lyophilization method reduced CFU counts in tissue and on implants compared to control groups; however, CFUs were still detected [51]. In this investigation, the absence of CFUs detected in tissue and on implants may be attributed to the enhanced drug loading of gentamicin achieved through EPD as opposed to the lyophilization method.

Yang et al. utilized implants in vivo with TNTs measuring 80 nm in diameter [51]. In their prior in vitro studies, lyophilization was used to load gentamicin on one side of a disc with a 10 mm diameter (surface area: 78.5 mm^2), achieving a cumulative gentamicin release of 91.45 μg over 57 h [52], which corresponds to 1.2 $\mu g/mm^2$ of gentamicin release relative to surface area. In contrast, our protocol produces TNTs with a diameter of 100 nm and enhances gentamicin localization above and within the TNT surface by combining chitosan with gentamicin via EPD [18]. In previous in vitro studies, this EPD coating method on the surface of cylindrical TNT implants with a 0.6 mm diameter and a coated length of 11 mm (surface area: 21.3 mm^2) achieved gentamicin release rates of 486.0 μg over 54 h and 501.5 μg over 72 h [18], equating to 22.8–23.5 $\mu g/mm^2$ of release. Thus, compared to the lyophilization approach by Yang et al. our TNT implants loaded via EPD with chitosan and gentamicin may have an estimated 19-fold increase in gentamicin release per surface area over time.

Other factors, such as inoculation dose, strain of *S. aureus*, or location of inoculation, may also have contributed to the differences in CFU counts observed between Yang et al. and this current study at the implant and tissue at the study endpoints. In this study, consistent with the absence of CFUs detected in tissue and on implants, the chitosan + gentamicin group exhibited substantially reduced or absent secondary markers associated with infection, which included bacterial BLI signal, implant biofilm, periosteal reaction, peri-implant bone loss, bone inflammatory infiltrate, weight-loss, as well as pain behavior and weight-bearing assessments.

Bernthal et al. demonstrated a strong correlation between BLI signal intensity around the knee joint implant site and total ex vivo CFUs harvested from tissue and implants in a mouse PJI model using bioluminescent *S. aureus* ($R^2 = 0.9873$) [28]. In the present study, the chitosan + gentamicin group maintained BLI signal intensity at or below baseline levels at all evaluated time points (Days 1, 3, 5, 7, 10, and 14) following surgery and inoculation. The baseline BLI signal was recorded before surgery and inoculation with bioluminescent *Xen36 S. aureus*. The lack of increase in BLI signal above baseline across these time points in the chitosan + gentamicin group supports the antimicrobial efficacy of the implants, further corroborated by the absence of detectable biofilm on the implant surface as observed by SEM imaging.

While there was an absence of detection of bacteria and biofilm, it is noteworthy that a mild-to-moderate periosteal reaction was observed in a few mice on Day 14 in the chitosan + gentamicin group on radiography. In a previous study using the same animal model, we found that mice receiving control uncoated femoral implants without bacterial inoculation often exhibited evidence of mild periosteal reaction on microcomputed tomography [27]. These findings indicate that trauma, a well-known mediator of periosteal reaction [53], from implant surgery itself induced an inflammatory response, leading to periosteal reaction. While this finding was evident on plain X-ray in a few mice in the chitosan + gentamicin group, periosteal reaction in this group was dramatically lower as compared to the chitosan group.

Pain, as well as joint dysfunction, are frequent symptoms in patients with PJI [54–56]. We evaluated these symptoms through assessments of mechanical allodynia and weight-bearing on the implant leg, both of which were improved in the chitosan + gentamicin group. By Day 14, all mice in the chitosan + gentamicin group exhibited full weight-bearing on the implant leg, and this group had no significant change in mechanical allodynia between baseline (Day 0) and Day 14.

A strength of this study is the use of a well-established mouse model of PJI [27–34] and the use of *S. aureus*, one of the most common pathogens isolated in patients with PJI [1–6]. A limitation is that only gentamicin was tested as an antimicrobial drug. Other antibiotics, such as vancomycin, could also be

utilized for EPD coating, which has previously been performed [57]. The implants in this study were not assessed for osseointegration capabilities. Our previous research indicated that a 24-h incubation period of these TNT implants coated with chitosan + gentamicin in culture did not negatively impact osteoblast viability in vitro [18]. In the present study, mice inoculated with *S. aureus* with TNT implants coated with chitosan + gentamicin showed minimal peri-implant bone loss and inflammatory infiltration around the implant site in the distal femur, as observed in H&E-stained sections at Day 14. This observation was consistent with our previous findings in the control group of the mouse model without bacterial inoculation using stainless steel femoral implants [27].

Prior animal studies have demonstrated that implants with TNTs can enhance osseointegration [23–26]. Given the EPD coating applied to the TNT surface in this study, it is crucial to evaluate the osseointegration potential of these implants in vivo. We are currently conducting such evaluations and plan to extend these investigations in future studies. Furthermore, the capability of the implant surface and coating to withstand higher impact and abrasion forces, as seen in the clinical setting as opposed to a mouse surgical model, requires further exploration.

Another limitation is that we did not conduct an in-depth evaluation of adverse side effects from the implants. Mice were monitored daily and, based on our IACUC protocol, exhibited no physical or behavioral signs of pain or distress, as outlined in Supplementary Methods S1, necessitating euthanasia. Chitosan has an FDA generally recognized as safe (GRAS) status and is commonly used in dietary supplements and medical devices, such as wound dressings and gels [58]. The primary concerns regarding gentamicin-related adverse effects are nephrotoxicity and ototoxicity [59], which were not assessed in this study. In the clinical studies of gentamicin poly (D, L-lactide) orthopedic implant coatings have reported the benefit of delivering localized high concentrations of gentamicin directly to the target site, avoiding high systemic doses and systemic side effects, such as nephrotoxicity and ototoxicity [60, 61].

Another potential concern is local toxicity of the implant coating. Our previous studies showed no adverse effects on osteoblast viability with our coated implants in vitro [18]. Additionally, in this study, the surrounding bone tissue of mice with TNT-coated implants loaded with chitosan and gentamicin and inoculated with Xen36 *S. aureus* at surgery did not exhibit substantial bone pathology on histologic and X-ray analysis and was similar to what we observed in mice with bare stainless steel femoral implants without infection [27]. However, the present study offers a limited analysis of local adverse effects, an area we are actively investigating. This includes studies conducted in the absence of infection, using implants coated with the same gentamicin concentration as in the current investigation, as well as coatings with a tenfold lower gentamicin dose achieved by adjusting the voltage and duration in the EPD process.

5 | Conclusion

The application of Ti implants with TNTs coated with chitosan and gentamicin via EPD effectively prevented bacterial colonization on the implant and peri-implant tissue in a mouse model of PJI. This study presents preclinical evidence supporting the efficacy of a novel implant coating and localized antimicrobial delivery system for PJI prevention. Further research is needed to assess how implants with TNTs coated with chitosan and gentamicin via EPD would translate to clinical applications, particularly regarding their impact on osseointegration and overall performance as prosthetic devices.

Author Contributions

John L. Hamilton: conceptualization, formal analysis, funding, investigation, methodology, project administration, supervision, validation, visualization, writing–original draft preparation, writing–review and editing. **Sofia Gianotti:** investigation, writing–review and editing. **Julia Fischer:** investigation, writing–review and editing. **Greta Della Fara:** investigation, writing–review and editing. **Amandine Impergre:** investigation, writing–review and editing. **Francesca De Vecchi:** investigation, writing–review and editing. **Mohammed AbuAlia:** investigation. **Alfons Fischer:** methodology, resources, writing–review and editing. **Adrienn Markovics:** conceptualization, investigation, methodology, resources, writing–original draft preparation, writing–review and editing. **Markus A. Wimmer:** conceptualization, formal analysis, funding acquisition, resources, methodology, project administration, supervision, validation, visualization, writing–review and editing.

Acknowledgments

The Grainger Directorship of the Rush Arthritis and Orthopedics Institute (Markus A. Wimmer), NIH NIAMS R21 grant (R21AR084167) to John L. Hamilton and Markus A. Wimmer, and NIH NIAMS T32 grant (T32AR073157) to D. Rick Sumner provided funding during the study period.

Ethics Statement

This research received approval from the Rush University Medical Center Institutional Animal Care and Use Committee (IACUC No: 23-012). All procedures adhered to the standards outlined in the Guide for the Care and Use of Laboratory Animals (Institute of Laboratory Animal Resources, National Academy of Sciences, Bethesda, MD, USA).

Conflicts of Interest

John L. Hamilton, Markus A. Wimmer, Adrienn Markovics, and Greta Della Fara have filed a pending patent (PCT/US2023/018967) related to work associated with this study.

References

1. V. Aggarwal, H. Bakhshi, N. Ecker, J. Parvizi, T. Gehrke, and D. Kendoff, "Organism Profile in Periprosthetic Joint Infection: Pathogens Differ at Two Arthroplasty Infection Referral Centers in Europe and in the United States," *Journal of Knee Surgery* 27 (2014): 399–406.

2. L. Pulido, E. Ghanem, A. Joshi, J. J. Purtill, and J. Parvizi, "Periprosthetic Joint Infection: The Incidence, Timing, and Predisposing Factors," *Clinical Orthopaedics & Related Research* 466 (2008): 1710–1715.

3. L. Manning, S. Metcalf, B. Clark, et al., "Clinical Characteristics, Etiology, and Initial Management Strategy of Newly Diagnosed Periprosthetic Joint Infection: A Multicenter, Prospective Observational Cohort Study of 783 Patients," *Open Forum Infectious Diseases* 7 (2020): ofaa068.

4. Y. Tsai, C. H. Chang, Y. C. Lin, S. H. Lee, P. H. Hsieh, and Y. Chang, "Different Microbiological Profiles Between Hip and Knee Prosthetic Joint Infections," *Journal of Orthopaedic Surgery* 27 (2019): 230949 9019847768.

5. N. Benito, I. Mur, A. Ribera, et al., "The Different Microbial Etiology of Prosthetic Joint Infections According to Route of Acquisition and Time After Prosthesis Implantation, Including the Role of Multidrug-Resistant Organisms," *Journal of Clinical Medicine* 8 (2019): 673.

6. E. J. Weinstein, A. J. Stephens-Shields, C. W. Newcomb, et al., "Incidence, Microbiological Studies, and Factors Associated With Prosthetic Joint Infection After Total Knee Arthroplasty," *JAMA Network Open* 6 (2023): e2340457.

7. S. Tarabichi, A. F. Chen, C. A. Higuera, et al., "2022 American Association of Hip and Knee Surgeons Symposium: Periprosthetic Joint Infection," *Journal of Arthroplasty* 38 (2023): S45–S49.

8. C. N. Carender, K. M. Fruth, D. G. Lewallen, D. J. Berry, M. P. Abdel, and N. A. Bedard, "Obesity and Primary Total Hip Arthroplasty: The Absolute Versus Relative Risk of Periprosthetic Joint Infection at 15 Years," *Journal of Arthroplasty* 39 (2024): S436–S443.e1.

9. X. Jin, B. Gallego Luxan, M. Hanly, et al., "Estimating Incidence Rates of Periprosthetic Joint Infection After Hip and Knee Arthroplasty for Osteoarthritis Using Linked Registry and Administrative Health Data," *Bone & Joint Journal* 104–B (2022): 1060–1066.

10. J. S. M. Mortazavi, J. Schwartzenberger, M. S. Austin, J. J. Purtill, and J. Parvizi, "Revision Total Knee Arthroplasty Infection: Incidence and Predictors," *Clinical Orthopaedics & Related Research* 468 (2010): 2052–2059.

11. H. Abdelaziz, R. Jaramillo, T. Gehrke, M. Ohlmeier, and M. Citak, "Clinical Survivorship of Aseptic Revision Total Knee Arthroplasty Using Hinged Knees and Tantalum Cones at Minimum 10-Year Follow-Up," *Journal of Arthroplasty* 34 (2019): 3018–3022.

12. A. H. Goldman, D. R. Osmon, A. D. Hanssen, M. W. Pagnano, D. J. Berry, and M. P. Abdel, "Aseptic Reoperations Within 1 Year of Primary Total Knee Arthroplasty Markedly Increase the Risk of Later Periprosthetic Joint Infection," *Journal of Arthroplasty* 35 (2020): 3668–3672.

13. E. Beam and D. Osmon, "Prosthetic Joint Infection Update," *Infectious Disease Clinics of North America* 32 (2018): 843–859.

14. Z. C. Lum, K. M. Natsuhara, T. J. Shelton, M. Giordani, G. C. Pereira, and J. P. Meehan, "Mortality During Total Knee Periprosthetic Joint Infection," *Journal of Arthroplasty* 33 (2018): 3783–3788.

15. K. M. Natsuhara, T. J. Shelton, J. P. Meehan, and Z. C. Lum, "Mortality During Total Hip Periprosthetic Joint Infection," *Journal of Arthroplasty* 34 (2019): S337–S342.

16. A. Premkumar, D. A. Kolin, K. X. Farley, et al., "Projected Economic Burden of Periprosthetic Joint Infection of the Hip and Knee in the United States," *Journal of Arthroplasty* 36 (2021): 1484–1489-e1483.

17. V. Alt, "Antimicrobial Coated Implants in Trauma and Orthopaedics-A Clinical Review and Risk-Benefit Analysis," *Injury* 48 (2017): 599–607.

18. G. Della Fara, A. Markovics, S. Radice, et al., "Electrophoretic Deposition of Gentamicin and Chitosan Into Titanium Nanotubes to Target Periprosthetic Joint Infection," *Journal of Biomedical Materials Research, Part B: Applied Biomaterials* 111 (2023): 1697–1704.

19. A. Pawlik, M. Jarosz, K. Syrek, and G. D. Sulka, "Co-Delivery of Ibuprofen and Gentamicin From Nanoporous Anodic Titanium Dioxide Layers," *Colloids and Surfaces B: Biointerfaces* 152 (2017): 95–102.

20. M. Kaur and K. Singh, "Review on Titanium and Titanium Based Alloys as Biomaterials for Orthopaedic Applications," *Materials Science & Engineering, C: Materials for Biological Applications* 102 (2019): 844–862.

21. U. Diebold, "Structure and Properties of TiO_2 Surfaces: A Brief Review," *Applied Physics A: Materials Science & Processing* 76 (2003): 681–687.

22. K. Gulati, M. S. Aw, and D. Losic, "Drug-Eluting Ti Wires With Titania Nanotube Arrays for Bone Fixation and Reduced Bone Infection," *Nanoscale Research Letters* 6 (2011): 571.

23. L. M. Bjursten, L. Rasmusson, S. Oh, G. C. Smith, K. S. Brammer, and S. Jin, "Titanium Dioxide Nanotubes Enhance Bone Bonding in Vivo," *Journal of Biomedical Materials Research. Part A* 92 (2010): 1218–1224.

24. N. Wang, H. Li, W. Lü, et al., "Effects of TiO_2 Nanotubes With Different Diameters on Gene Expression and Osseointegration of Implants in Minipigs," *Biomaterials* 32 (2011): 6900–6911.

25. J. Wang, F. Meng, W. Song, et al., "Nanostructured Titanium Regulates Osseointegration via Influencing Macrophage Polarization in the Osteogenic Environment," *International Journal of Nanomedicine* 13 (2018): 4029–4043.

26. E. P. Su, D. F. Justin, C. R. Pratt, et al., "Effects of Titanium Nanotubes on the Osseointegration, Cell Differentiation, Mineralisation and Antibacterial Properties of Orthopaedic Implant Surfaces," *Bone & Joint Journal* 100–B (2018): 9–16.

27. J. Hamilton, M. Mohamed, B. Witt, M. Wimmer, and S. Shafikhani, "Therapeutic Assessment of N-Formyl-Methionyl-Leucyl-Phenylalanine (fMLP) in Reducing Periprosthetic Joint Infection," *European Cells and Materials* 42 (2021): 122–138.

28. N. M. Bernthal, A. I. Stavrakis, F. Billi, et al., "A Mouse Model of Post-Arthroplasty *Staphylococcus aureus* Joint Infection to Evaluate in Vivo the Efficacy of Antimicrobial Implant Coatings," *PLoS One* 5 (2010): e12580.

29. J. A. Niska, J. H. Shahbazian, R. I. Ramos, K. P. Francis, N. M. Bernthal, and L. S. Miller, "Vancomycin-Rifampin Combination Therapy Has Enhanced Efficacy Against an Experimental *Staphylococcus aureus* Prosthetic Joint Infection," *Antimicrobial Agents and Chemotherapy* 57 (2013): 5080–5086.

30. V. Hegde, E. M. Dworsky, A. I. Stavrakis, et al., "Single-Dose, Preoperative Vitamin-D Supplementation Decreases Infection in a Mouse Model of Periprosthetic Joint Infection," *Journal of Bone and Joint Surgery* 99 (2017): 1737–1744.

31. N. M. Bernthal, B. N. Taylor, J. A. Meganck, et al., "Combined in Vivo Optical and MicroCT Imaging to Monitor Infection, Inflammation, and Bone Anatomy in an Orthopaedic Implant Infection in Mice," *Journal of Visualized Experiments* 446, no. 92 (2014): e51612.

32. J. M. Thompson, V. Saini, A. G. Ashbaugh, et al., "Oral-Only Linezolid-Rifampin Is Highly Effective Compared With Other Antibiotics for Periprosthetic Joint Infection: Study of a Mouse Model," *Journal of Bone and Joint Surgery* 99 (2017): 656–665.

33. A. I. Stavrakis, S. Zhu, V. Hegde, et al., "In Vivo Efficacy of a 'Smart' Antimicrobial Implant Coating," *Journal of Bone and Joint Surgery* 98 (2016): 1183–1189.

34. J. R. Pribaz, N. M. Bernthal, F. Billi, et al., "Mouse Model of Chronic Post-Arthroplasty Infection: Noninvasive in Vivo Bioluminescence Imaging to Monitor Bacterial Burden for Long-Term Study," *Journal of Orthopaedic Research* 30 (2012): 335–340.

35. N. M. Bernthal, J. R. Pribaz, A. I. Stavrakis, et al., "Protective Role of IL-1β Against Post-Arthroplasty *Staphylococcus aureus* Infection," *Journal of Orthopaedic Research* 29 (2011): 1621–1626.

36. C. Kilkenny, W. J. Browne, I. C. Cuthill, M. Emerson, and D. G. Altman, "Improving Bioscience Research Reporting: The ARRIVE Guidelines for Reporting Animal Research," *PLoS Biology* 8 (2010): e1000412.

37. J. Goldufsky, S. J. Wood, V. Jayaraman, et al., "*Pseudomonas aeruginosa* Uses T3SS to Inhibit Diabetic Wound Healing," *Wound Repair and Regeneration* 23 (2015): 557–564.

38. J. S. Kroin, A. Buvanendran, J. Li, et al., "Short-Term Glycemic Control Is Effective in Reducing Surgical Site Infection in Diabetic Rats," *Anesthesia and Analgesia* 120 (2015): 1289–1296.

39. J. S. Kroin, A. Buvanendran, K. J. Tuman, and J. M. Kerns, "Effect of Acute Versus Continuous Glycemic Control on Duration of Local

Anesthetic Sciatic Nerve Block in Diabetic Rats," *Regional Anesthesia and Pain Medicine* 37 (2012): 595–600.

40. J. S. Kroin, J. Li, J. W. Goldufsky, et al., "Perioperative High Inspired Oxygen Fraction Therapy Reduces Surgical Site Infection With *Pseudomonas aeruginosa* in Rats," *Journal of Medical Microbiology* 65 (2016): 738–744.

41. J. S. Kroin, J. Li, S. Shafikhani, et al., "Local Vancomycin Effectively Reduces Surgical Site Infection at Implant Site in Rodents," *Regional Anesthesia and Pain Medicine* 43 (2018): 795–804.

42. A. V. Carli, S. Bhimani, X. Yang, et al., "Quantification of Peri-Implant Bacterial Load and in Vivo Biofilm Formation in an Innovative, Clinically Representative Mouse Model of Periprosthetic Joint Infection," *Journal of Bone and Joint Surgery American* 99 (2017): e25.

43. H. J. Im, J. S. Kim, X. Li, et al., "Alteration of Sensory Neurons and Spinal Response to an Experimental Osteoarthritis Pain Model," *Arthritis & Rheumatism* 62 (2010): 2995–3005.

44. R. E. Miller, P. B. Tran, R. Das, et al., "CCR2 Chemokine Receptor Signaling Mediates Pain in Experimental Osteoarthritis," *Proceedings of the National Academy of Sciences United States of America* 109 (2012): 20602–20607.

45. T. W. Bauer, J. Parvizi, N. Kobayashi, et al., "Diagnosis of Periprosthetic Infection," *Journal of Bone and Joint Surgery-American Volume* 88 (2006): 869–882.

46. K. M. Kruszewski, L. Nistico, M. J. Longwell, et al., "Reducing *Staphylococcus aureus* Biofilm Formation on Stainless Steel 316L Using Functionalized Self-Assembled Monolayers," *Materials Science & Engineering C: Materials for Biological Applications* 33 (2013): 2059–2069.

47. M. Kazemzadeh-Narbat, B. F. L. Lai, C. Ding, J. N. Kizhakkedathu, R. E. W. Hancock, and R. Wang, "Multilayered Coating on Titanium for Controlled Release of Antimicrobial Peptides for the Prevention of Implant-Associated Infections," *Biomaterials* 34 (2013): 5969–5977.

48. S. A. Shehadat, M. O. Gorduysus, S. S. A. Hamid, N. A. Abdullah, A. R. Samsudin, and A. Ahmad, "Optimization of Scanning Electron Microscope Technique for Amniotic Membrane Investigation: A Preliminary Study," *European Journal of Dentistry* 12 (2018): 574–578.

49. R. O. Darouiche, "Treatment of Infections Associated With Surgical Implants," *New England Journal of Medicine* 350 (2004): 1422–1429.

50. J. W. Costerton, P. S. Stewart, and E. P. Greenberg, "Bacterial Biofilms: A Common Cause of Persistent Infections," *Science* 284 (1999): 1318–1322.

51. Y. Yang, H. Y. Ao, S. B. Yang, et al., "In Vivo Evaluation of the Anti-Infection Potential of Gentamicin-Loaded Nanotubes on Titania Implants," *International Journal of Nanomedicine* 11 (2016): 2223–2234.

52. W. T. Lin, H. L. Tan, Z. L. Duan, et al., "Inhibited Bacterial Biofilm Formation and Improved Osteogenic Activity on Gentamicin-Loaded Titania Nanotubes With Various Diameters," *International Journal of Nanomedicine* 9 (2014): 1215–1230.

53. R. S. Rana, J. S. Wu, and R. L. Eisenberg, "Periosteal Reaction," *American Journal of Roentgenology* 193 (2009): W259–W272.

54. P. Izakovicova, O. Borens, and A. Trampuz, "Periprosthetic Joint Infection: Current Concepts and Outlook," *EFORT Open Reviews* 4 (2019): 482–494.

55. A. L. L. Lima, P. R. Oliveira, V. C. Carvalho, E. S. Saconi, H. B. Cabrita, and M. B. Rodrigues, "Periprosthetic Joint Infections," *Interdisciplinary Perspectives on Infectious Diseases* 2013 (2013): 542796.

56. S. Bozhkova, V. Suardi, H. K. Sharma, et al., "The W.A.I.O.T. Definition of Peri-Prosthetic Joint Infection: A Multi-Center, Retrospective Validation Study," *Journal of Clinical Medicine* 9 (2020): 1965.

57. F. Ordikhani, E. Tamjid, and A. Simchi, "Characterization and Antibacterial Performance of Electrodeposited Chitosan-Vancomycin Composite Coatings for Prevention of Implant-Associated Infections," *Materials Science & Engineering, C: Materials for Biological Applications* 41 (2014): 240–248.

58. S. Jesus, A. P. Marques, A. Duarte, et al., "Chitosan Nanoparticles: Shedding Light on Immunotoxicity and Hemocompatibility," *Frontiers in Bioengineering and Biotechnology* 8 (2020): 100.

59. H. Mattie, W. A. Craig, and J. C. Pechèré, "Determinants of Efficacy and Toxicity of Aminoglycosides," *Journal of Antimicrobial Chemotherapy* 24 (1989): 281–293.

60. T. Fuchs, R. Stange, G. Schmidmaier, and M. J. Raschke, "The Use of Gentamicin-Coated Nails in the Tibia: Preliminary Results of a Prospective Study," *Archives of Orthopaedic and Trauma Surgery* 131 (2011): 1419–1425.

61. W. J. Metsemakers, M. Reul, and S. Nijs, "The Use of Gentamicin-Coated Nails in Complex Open Tibia Fracture and Revision Cases: A Retrospective Analysis of a Single Centre Case Series and Review of the Literature," *Injury* 46 (2015): 2433–2437.

Supporting Information

Additional supporting information can be found online in the Supporting Information section.